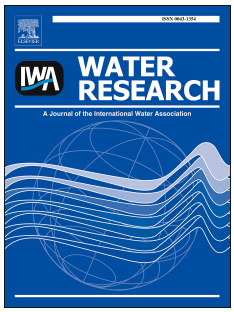

The formation of a metalimnetic oxygen minimum exemplifies how ecosystem dynamics shape biogeochemical processes: A modelling study

Chenxi Mi, Tom Shatwell, Jun Ma, Valerie Carolin Wentzky, Bertram Boehrer, Yaqian Xu, Karsten Rinke

PII: S0043-1354(20)30237-2

DOI: https://doi.org/10.1016/j.watres.2020.115701

Reference: WR 115701

To appear in: *Water Research*

Received Date: 10 June 2019

Revised Date: 14 January 2020

Accepted Date: 6 March 2020

Please cite this article as: Mi, C., Shatwell, T., Ma, J., Wentzky, V.C., Boehrer, B., Xu, Y., Rinke, K., The formation of a metalimnetic oxygen minimum exemplifies how ecosystem dynamics shape biogeochemical processes: A modelling study, *Water Research* (2020), doi: https://doi.org/10.1016/j.watres.2020.115701.

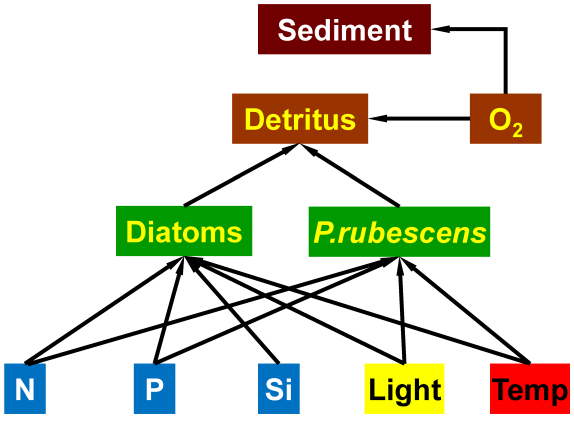

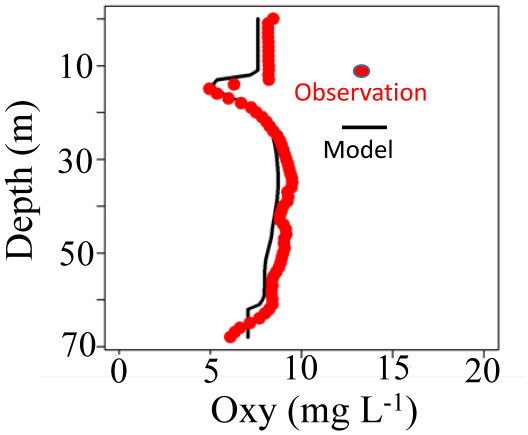

Title Page

Title:

The formation of a metalimnetic oxygen minimum exemplifies how ecosystem dynamics shape biogeochemical processes: A modelling study

Chenxi Mi[1,2,*], Tom Shatwell[1], Jun Ma[3], Valerie Carolin Wentzky[1,4], Bertram Boehrer[1], Yaqian Xu[3], Karsten Rinke[1]

[1] Helmholtz Centre for Environmental Research, Department of Lake Research, Magdeburg, Germany

[2] College of Water Conservancy, Shenyang Agricultural University, Shenyang, China

[3]Hubei Key Laboratory of Ecological Restoration of River-Lakes and Algal Utilization, Hubei University of Technology, Wuhan, China

[4] State Agency for Agriculture, Environment and Rural Areas Schleswig-Holstein (LLUR), 24220 Flintbek, Germany

*corresponding author

Title:

The formation of a metalimnetic oxygen minimum exemplifies how ecosystem dynamics shape biogeochemical processes: A modelling study

Abstract

Metalimnetic oxygen minima are observed in many lakes and reservoirs, but the mechanisms behind this phenomena are not well understood. Thus, we simulated the metalimnetic oxygen minimum (MOM) in the Rappbode Reservoir with a well-established two-dimensional water quality model (CE-QUAL-W2) to systematically quantify the chain of events leading to its formation. We used high-resolution measured data to calibrate the model, which accurately reproduced the physical (e.g. water level and water temperature), biogeochemical (e.g. nutrient and oxygen dynamics) and ecological (e.g. algal community dynamics) features of the reservoir, particularly the spatial and temporal extent of the MOM. The results indicated that around 60% of the total oxygen consumption rate in the MOM layer originated from benthic processes whereas the remainder originated from pelagic processes. The occurrence of the cyanobacterium *Planktothrix rubescens* in the metalimnion delayed and slightly weakened the MOM through photosynthesis, although its decaying biomass ultimately induced the MOM. Our research also confirmed the decisive role of water temperature in the formation of the MOM since the water temperatures, and thus benthic and pelagic oxygen consumption rates, were higher in the metalimnion than in the hypolimnion. Our model is not only providing novel conclusions about the drivers of MOM development

and their quantitative contributions, it is also a new tool for understanding and predicting ecological and biogeochemical water quality dynamics.

Keywords: Rappbode Reservoir; CE-QUAL-W2; *Planktothrix rubescens*; Metalimnion; Oxygen consumption; Benthic processes

1. Introduction

The concentration of dissolved oxygen (DO) is a key factor for surface water quality and significantly influences biogeochemical cycling in aquatic ecosystems (Rhodes et al. 2017; Terry et al. 2017; Zhang et al. 2015). For example, DO concentration directly affects growth and survival of aquatic organisms as well as predator-prey interactions (Wang et al. 1978). Oxygen interacts with the retention and release of phosphorus in the sediment and can influence the trophic status of lakes and reservoirs (Hupfer and Lewandowski 2008; Kang et al. 2018). Due to the importance of DO on aquatic ecosystems, it is not surprising that many investigations have focused on its dynamics and influencing factors.

Many recent studies have reported a decline in DO concentration in temperate stratified standing waters. Foley et.al (2012) analysed the long-term observations of Blelham Tarn, a monomictic lake in England, and found that hypolimnetic anoxia (the duration of hypolimnetic DO concentration <1g O_2 m^{-3}) of the lake extended by nearly three months

between 1966 and 2007. Knoll et al. (2018) found that the minimum oxygen concentration in the hypolimnion of an oligotrophic lake declined by 4.4 mg/l within 27 years. As a consequence of climate warming, deep-water oxygen content in several perialpine lakes decreased significantly between 1992 and 2016 (Rogora et al. (2018). All these studies focused on oxygen depletion in the hypolimnion and the mechanisms involved were fully characterised. In contrast, little attention has been paid to DO loss within the metaliminon and the occurrence of metalimnetic oxygen minima (hereafter MOM) is far less understood.

The metalimnion is the layer of high temperature and density gradients at the transition between the upper continuously mixing epilimnion and the hypolimnion. The occurrence of MOMs is affecting aquatic biogeochemistry, limnetic communities and has been described in many lakes and reservoirs worldwide (Wetzel 2001). A MOM forms a barrier for many organisms and therefore influences the vertical distribution and biomass production of invertebrates (Horppila et al. 2000) and fish (Liljendahl-Nurminen et al. 2008). Rice et al. (2013) illustrated that metalimnetic hypoxia can cause fish kills in Lake Norman. Additionally, McClure et al. (2018) reported the occurrence of MOM in the Falling Creek Reservoir and indicated that the phenomenon can significantly change greenhouse gas dynamics. In drinking water reservoirs, a MOM can induce water quality deteriorations due to release of manganese or other unwanted substances and may require management interventions.

MOMs form where vertical turbulent diffusion rates are low because this restricts the replenishment of oxygen from the water above or below (Kreling et al. 2017). Scientists disagree about the mechanisms triggering the phenomenon and several hypotheses have been

put forward. Early work by Shapiro (1960) illustrated that the respiration of copepods is the main driver of metalimnetic oxygen depletion in Lake Washington. Later research by Nix (1981) indicated that the high oxygen consumption in the metalimnion of DeGray Reservoir, USA, could be attributed to the entrainment of inflows with high loads of reduced substances (e.g. iron, manganese). A recent study by Müller et al. (2012) pointed out that rapid decomposition of organic materials sinking from the epilimnion may also play an important role in pelagic oxygen dynamics. As indicated by Kreling et al. (2017), however, many limnologists question these hypotheses, which currently remain speculation rather than explanation.

The metalimnion is characterized by very strong local gradients in temperature, biomass, microbial activity and transport rates of gas and solutes. This makes it extremely difficult to empirically quantify the different processes that contribute to MOM formation. Coupled hydrodynamic-ecological models are well-suited to analyze and explain the mechanisms of DO depletion and predict its future evolution (Elliott 2012; Hamilton and Schladow 1997; Ladwig et al. 2018) because they can simultaneously resolve transport and reactive processes. A detailed review of lake models by Arhonditsis and Brett (2004) concluded that predictive abilities for DO are high in comparison to biological variables (e.g. algae). More than 160 papers have been published in this field during the past 20 years (Web of Science search on the topic: lake & oxygen depletion & model). However, as stated above, most of these studies focused on modelling the depletion of hypolimnetic DO, and simulating the oxygen loss in the metalimnion remains a challenge (Weber et al. 2017). Joehnk and Umlauf (2001) presented a study about simulating the MOM in Lake Ammer using a one-dimensional (1D)

112 physical–ecological coupled model. They assumed that temperature-dependent biological
113 oxygen demand (BOD) and stratification duration were the main factors contributing to
114 MOM development. Antonopoulos and Gianniou (2003) followed a similar approach to
115 simulate the MOM in Lake Vegoritis and suggested that the vertical turbulent diffusivity (K_z)
116 had a big influence on metalimnetic DO dynamics. However, none of these models resolved
117 other ecosystem components like phytoplankton or nutrient dynamics and thus were unable to
118 link DO dynamics to ecosystem dynamics. Hence, the results from such model studies are not
119 easily transferable to other systems and unsuited to identify the drivers responsible for the
120 DO depletion. We therefore argue for the development of an advanced water quality model
121 that fully describes the ecological processes related to the MOM, including autotrophic and
122 heterotrophic ecosystem processes, to improve our understanding of the mechanisms behind
123 this phenomenon.

124 In this publication, we used a well-established water quality model (CE-QUAL-W2)
125 with a spatially explicit representation of hydrodynamics, oxygen, nutrients and
126 phytoplankton community dynamics to simulate the MOM in the Rappbode Reservoir
127 (Germany). In a previous study, the spatio-temporal dynamics of a MOM in the reservoir
128 were studied in great detail, providing empirical evidence that a bloom of the cyanobacterium
129 *Planktothrix rubescens* (hereafter *P. rubescens*) in the metalimnion provides an important
130 contribution for the formation of the MOM (Wentzky et al. 2019). Our model-based systems
131 analysis with closed dynamic budgets of oxygen, nutrients, and organic carbon allows us to
132 quantify the contribution of *P. rubescens* to the MOM. We were interested in finding out
133 whether MOMs can also emerge without metalimnetic phytoplankton mass developments.

For this purpose, we employed an experimental modelling approach (Mooij et al. 2010) and systematically studied, and quantified, the chain of events leading to the formation of the MOM. Beyond Wentzky et al. (2019), who proved the important contribution of pelagic oxygen depletion, we include sediment oxygen demand in our model and attempt to put both in relation to each other for Rappbode Reservoir. Besides this focused research question, we also strive to develop a template for an ecological lake model that can capture the dominant physical and biogeochemical processes in the metalimnion and predict metalimnetic dynamics.

2. Methods

2.1. Study site

Rappbode Reservoir is located in the eastern Harz Mountains and has a maximum depth of 89 m (Figure 1). It is the core of the Rappbode system, a network of 6 reservoirs used for flood protection, environmental flows, hydropower, recreation and drinking water supply. The reservoir was constructed in 1959 and it was filled to capacity by 1964. It is the largest drinking water reservoir in Germany, supplying drinking water to more than 1 million people (Mi et al. 2019). It receives water from two tributaries (Hassel and Rappbode pre-reservoirs) and a transfer gallery from Königshütte Reservoir. The water of the Rappbode Reservoir is discharged downstream into Wendefurth Reservoir (Rinke et al. 2013). The reservoir is a typical dimictic water body which stratifies in summer and winter and mixes completely in spring and autumn. Analysis of long-term monitoring data showed that the reduced use of

158 phosphate-containing detergents strongly decreased the phosphorus concentration in the
159 reservoir after 1991, which decreased the total phosphorus concentration during the mixing
160 period from 0.163 mg L^{-1} to 0.027 mg L^{-1}, and shifted the reservoir from a eutrophic to a
161 mesotrophic state (Wentzky et al. 2018). This strong decrease of phosphorus, however, did
162 not reduce the phytoplankton biomass, for which the annual mean biovolume was 1.164 mg
163 L^{-1} based on long-term measurements from 1971-2016 (Wentzky et al. 2018).
164

165 **2.2. Numerical model**

166 The two-dimensional (longitudinal-vertical) hydrodynamic and water quality model
167 CE-QUAL-W2 (hereafter W2) was selected for this study. The US Army Corps of Engineers
168 first launched the model in 1975 and the Department of Civil and Environmental Engineering
169 at Portland State University currently maintains and updates it. W2 has been successfully
170 used in simulating hydrodynamic and biogeochemical processes including the relationships
171 between temperature, nutrients, algae, dissolved oxygen, organic matter, and sediment for
172 different water bodies worldwide (Chang et al. 2015; Chong et al. 2018; Chuo et al. 2019;
173 Kobler et al. 2018; Sadeghian et al. 2018). A brief description of the relevant processes in
174 oxygen dynamics in W2 is provided below but for more detailed information about the model,
175 readers are referred to the user manual (Cole and Wells 2006) and an active user forum
176 (https://w2forum.cee.pdx.edu/). In our study, the hydrodynamic (water level and water
177 temperature) and water quality (two algae groups, nutrients and dissolved oxygen) modules
178 were used.

179 Oxygen is produced by photosynthesis of the two phytoplankton groups, whose

photosynthetic rates depend on available light and nutrients (phosphate, nitrate, ammonium for both groups, silicate only for diatoms). Vertical light attenuation follows Lambert-Beers law and includes algal self-shading, i.e. the overall light extinction coefficient is calculated by a background extinction coefficient plus the specific absorption cross-section of the two phytoplankton groups multiplied by their respective biomasses. Oxygen consumption in the model depends on phytoplankton respiration, decaying dissolved and particulate organic matter (which are imported by inflows and produced through phytoplankton mortality), through nitrification of ammonia, and through sediment consumption. The decay of organic matter is also linked to regeneration of nutrients. To account for sediment oxygen consumption and anoxic sediment release of phosphate and ammonium, a zero-order sediment compartment was included in the model, as has been reported in recent studies with a similar topic (Brito et al. 2018; Chong et al. 2018; Terry et al. 2017). Since the 2-D model is discretized into grid cells in the longitudinal and vertical directions, each grid cell is homogeneous in the lateral direction, and contains a sediment surface and a water volume in accordance with the bathymetry of the reservoir. Accordingly, in each 2D grid cell sediment oxygen consumption plays a role to some extent and the model explicitly accounts for oxygen consumption from both littoral and profundal sediments. In view of the research objective and limitation of observational data, other compartments like zooplankton, epiphyton, or macrophytes were not included in the model.

In this study, the latest version of W2 (V4.1) was used to simulate Rappbode Reservoir. W2 is suited for the reservoir because of its long, narrow and deep shape, for which the lateral gradients in both hydrodynamic and water quality variables can be neglected (see

Figure 1). The computational grid was built based on the hypsographic data provided by the reservoir authority (Talsperrenbetrieb Sachsen-Anhalt). The bathymetry input file contains four branches, including two branches for side arms so that the physical structure of the reservoir could be well represented by the model domain (Figure S1). In total, the reservoir was split into 106 segments along the longitudinal direction. The horizontal grid spacing ranged from 100 m to 400 m in the longitudinal direction and 5 m to 700 m in the lateral direction, whereas the vertical grid spacing was always 1 m. Overall, the full spatial model domain consisted of 3976 model cells. The grid-based elevation-volume relationship matched well with the observed bathymetry.

2.3. Model setup and input data

The boundary conditions for running W2 include time-series of meteorological input, inflow (including discharge, water temperature, nutrients) and outflow discharge. The meteorological input data include wind speed, air temperature, wind direction, shortwave radiation, cloud cover fraction and dew point temperature. The first four items were obtained from a monitoring buoy installed in the central part of the Rappbode Reservoir (see Rinke et al. 2013). High-frequency observations (every 10 minutes) were averaged to hourly values for driving the model. The very few missing values were filled by measurements from a nearby monitoring station at the Rappbode pre-reservoir (Friese et al. 2014; Rinke et al. 2013). Cloud cover fraction data were taken from the Harzgerode station of the German Weather Service (15 km away from the research area). Dew point temperatures were calculated from relative humidity and air temperature by the following equation (Bolton

1980):

$$T_{dp} = \frac{\lambda\left(ln\left(\frac{RH}{100}\right)+\frac{\beta T}{\lambda+T}\right)}{\beta-\left(ln\left(\frac{RH}{100}\right)+\frac{\beta T}{\lambda+T}\right)} \quad (1)$$

where T_{dp} is the dew point temperature (in °C), RH is the relative humidity (in %), T is the air temperature (in °C), and $\lambda = 237.7$°C and $\beta = 17.27$ are constants.

The daily inflow and outflow discharges were provided by the reservoir authority of the state of Saxony-Anhalt (Talsperrenbetrieb Sachsen-Anhalt), inflow water temperatures were drawn from a YSI-6200 probe at the pre-reservoirs and Königshütte Reservoir (see Rinke et al. 2013). Inflow nutrients (nitrate, ammonia, orthophosphate, silicate) were measured at biweekly resolution by continuous flow photometry (CFA, Skalar, The Netherlands) at the upstream stations of the Rappbode Reservoir (Friese et al. 2014).

The minimum time step for the simulation was set to 1 second as recommended to keep numerical stability. The output frequency of the simulation was one hour to enable sub-daily changes of hydrodynamic and water quality variables. Initial conditions (water level, water temperature, nutrients, algal and oxygen concentration) for starting the simulation were taken from measurements conducted at the deepest point of the reservoir (see Wentzky et al. 2018). Since the simulation started during deep recirculation in winter, a single vertical profile was used to initialize all horizontal segments.

2.4. Model calibration

The model was run and calibrated from January 19th to December 31st in 2016. This period was selected because this year showed a clear metalimnetic oxygen minimum, which

was covered by high quality observational data, for both stratification and water quality. The field data used for calibration were measured close to the dam wall (same location as for initial conditions) including: (1) daily water level, provided by the reservoir authority; (2) biweekly profiles of water temperature and dissolved oxygen, measured by a Hydrolab DS5 probe; (3) biweekly profiles of nutrient concentration (nitrate and silicate), measured by accredited methods following German standards (see Wentzky et al. 2018); (4) biweekly profiles of algae concentration (*P. rubescens* and diatoms), detected by a multi-channel fluorescence probe (FluoroProbe, bbe moldaenke GmbH). We separately determined the plankton composition by microscopic counts (for more information about differentiating algal groups from the fluorescence probe see Wentzky et al. (2019)). We did not calibrate ammonia or orthophosphate in the study, since most measurements in 2016 were below the detection limit (< 0.01 mg L^{-1} for ammonia, < 0.003 mg L^{-1} for orthophosphate). Model adjustment and calibration was realized in three steps, more details of the underlying procedures are given in the SI.

Step 1: Water budget

Deviations in the water budget could always be attributed to inaccurate input data of bathymetry, inflow and outflow discharge. We closed the water budget by incorporating a distributed tributary, as it was recommended in the manual of W2. A graphical illustration of this distributed inflow is given in Figure S2.

Step 2: Water temperatures

We only calibrated the wind sheltering coefficient by minimizing RMSE (see Table S1 in the SI for further details) and intentionally left all other internal hydrodynamics parameters

unchanged because they have a solid empirical basis (Mi et al. 2018). Note that the background extinction coefficient was not calibrated but determined based on *in situ* measurements. We set its value close to the minimum extinction coefficient that was observed in 2016 according to measurements of photosynthetically available radiation with two spherical LiCor LI-193SA light sensors (0.45 m^{-1}, see Supplementary Figure S4).

Step 3: Water quality model

We intentionally did not rely on computational optimization algorithms to parameterize the model. In our experience, such algorithms can produce a good model fit but can lead to over-optimized parameterizations with low transferability to other systems, biased results outside the optimized state space, and less explanatory power for systems analysis (Fenocchi et al. 2019). For instance, we initially used a semi-automated optimization procedure, which yielded a low model error for oxygen and good spatial and temporal representation of the MOM and chlorophyll concentration of diatoms and *P. rubescens*. However, this was based on biologically unrealistic parameter combinations, including very low pigment content and very high phosphorus affinity of *P. rubescens* compared to diatoms, combined with a low sediment oxygen demand. In our experience, as many parameters as possible should be determined *a priori* by expert knowledge and empirical evidence in order to incorporate ecological understanding of the important processes. This produces a more robust, transferable model, even at the expense of a slightly higher model error. The following empirical observations provided guidance for the specification of the ecological model: (i) a strong growth of diatoms in the epilimnion after the onset of stratification, (ii) subsequent full depletion of phosphate in the epilimnion and sedimentation of diatoms, (iii) appearance and

289 growth of *P. rubescens* in the metalimnion, and (iv) intense oxygen depletion in the
290 metalimnion coinciding with the disappearance of *P. rubescens*. Based on the different
291 ecological niches that spring diatoms and *P. rubescens* occupied in Rappbode Reservoir, we
292 parameterized spring diatoms as r-strategists with high maximum growth rates and moderate
293 light requirements, whereas we characterized *P. rubescens* as a k-strategist with slow growth
294 rate, low mortality rate due to grazing resistance, and an adaptation to low light and cold
295 regimes (Posch et al. 2012; Walsby and Jüttner 2006). By combination of literature values,
296 ecological expert knowledge and evaluation of historical data from Rappbode Reservoir, we
297 were able to *a priori* determine all parameters of the ecological model except the four key
298 parameters: AG#1, AG#2, ASAT#1, and ASAT#2 (see Table 1), which describe
299 light-dependent growth of both algal groups and required calibration. The details of this
300 calibration procedure as well as the description of the *a priori* parameterization are outlined
301 in the SI. Since the formation of a MOM was sensitive to sediment oxygen demand (SOD),
302 we independently estimated SOD in the hypolimnion from measured oxygen profiles using
303 the model of Livingstone and Imboden (1996) (see supplementary information and Figure S5
304 for details).

305 The coefficient of determination (R^2), root-mean-square-error (RMSE) and Nash
306 Sutcliffe efficiency (NSE) were used to measure model performance. These coefficients are
307 widely used to evaluate model performance (Carraro et al. 2012; Mi et al. 2018). We used
308 packages "tidyr", "Metrics" and "hydroGOF" in R version 3.4.3 to organize simulation output
309 data and for calculating RMSE and NSE.

310

2.5. Sensitivity analysis and model robustness

We performed a local sensitivity analysis (one by one parameter) of the ecological model by changing each parameter value (p), in Table 1, by ±5% and ±10% and calculated specific sensitivity coefficients (*SSC*, see Rangel-Peraza et al. (2016)) for the minimum oxygen concentrations in the MOM (DO_{min}) as:

$$SSC = \frac{\frac{DO_{min,mod} - DO_{min,ref}}{DO_{min,ref}}}{\frac{p_{mod} - p_{ref}}{p_{ref}}}$$

Here the indices *ref* and *mod* stand for reference and modified parameter settings, respectively. After evaluating the four parameter changes for each parameter, we averaged the *SSC* values in order to achieve an average sensitivity result at the local vicinity of each parameter value. We defined DO_{min} as the global minimum DO concentration in the top 35m of the reservoir. The three parameters AT1, AHSSI#1 and SODK2 were not included because AT1 for diatoms and AHSSI#1 were 0 and it makes no sense to change them on a percentage scale and SODK2 in the reference simulation is 0.99 which is not allowed to be higher than 1.

We used the same set of simulations for a robustness assessment and evaluated the characteristics of the MOM under the various parameter perturbations in order to analyze the robustness of the MOM phenomenon with respect to our parameterization. For each simulation, we analyzed the value of $DO_{min,35m}$, the depth of $DO_{min,35m}$, as well as the difference in DO concentration between the minimum and 8 m below and above (taken at the day in which the minimum occurs).

2.6. Model system analysis

We used the calibrated model to investigate the contributions of pelagic (P. rubescens and diatoms) and benthic processes (SOD) to the formation of the MOM by hierarchical model experiments, where different processes were turned off and compared to the reference simulation (scenario A) obtained with the calibrated model. We firstly switched off only the module of *P. rubescens* (scenario B), and then only the diatoms (scenario C), respectively, to quantify the contribution of these two algal groups to the MOM. Subsequently, we switched off both algal modules simultaneously (scenario D) to check the total influence of pelagic processes on the MOM. In order to test the contribution of benthic processes to MOM formation we turned off the SOD module and left both algal groups active (scenario E). Finally, as a control treatment, we run the model without algae and without SOD.

3. Results

3.1. Model performance and goodness of fit

The parameters used in the calibrated model are shown in Table 1. An additional distributed inflow with a small discharge (yearly mean value of 0.05 $m^3 s^{-1}$) was incorporated into the simulation in order to close the water budget. The simulated water level agreed well with the observations (RMSE = 0.03 m, R^2 = 0.99, NSE=0.99; see Figure S3). The simulated water temperatures were also in excellent agreement with the measurements (RMSE = 0.45 °C, R^2 = 0.99, NSE=0.99; Figure 2) including the dynamics in thermocline depth indicating an accurate reproduction of the hydrodynamic processes in the reservoir. The

simulated timing of stratification onset and autumnal mixing also agreed well with the observed data (Figure 2).

The model adequately captured the dynamics of the two algal groups (see Figure 3). The R^2 values for both *P. rubescens* and diatoms were above 0.5 (Table 2) and the model well reproduced the spring diatom bloom as well as the autumnal metalimnetic bloom of *P. rubescens* (see Figure 3). Although the model slightly underestimated the maximum concentration of *P. rubescens* in summer, it accurately captured the timing of the *P. rubescens* bloom (day 200 to 250), its vertical localization, as well as the gradual decline of the bloom from late August due to decreasing irradiance. The model satisfactorily captured the peak concentration (6.5 µg L^{-1}, given as chlorophyll *a*) of diatoms during spring but slightly underestimated the deep water concentrations in winter and spring.

The model also correctly predicted the nutrient concentrations (Table 2, Figure 4 and 5), with better performance for silicate (R^2 = 0.84) than for nitrate (R^2 = 0.69). Because of thermal stratification and strong depletion in the illuminated surface layers, the observed nutrient concentrations were always higher in the hypolimnion than in the epilimnion and the model reproduced this pattern. The simulated nitrate concentrations were slightly, but systematically lower than measurements resulting in a low value for NSE although the vertical gradients were well reproduced (Figure 4). The modeled silicate concentrations at the surface from late summer to early winter were slightly higher than the measurements (Figure 5).

The model accurately captured the observed oxygen dynamics (R^2 = 0.84), particularly the spatial and temporal extent of the MOM in the sampling location (Figure 6 and 7). In

accordance with the measurements, the formation of the MOM started at the end of July and the concentration decreased gradually to its lowest value in mid-September. Both the modeled and observed oxygen concentrations showed that the oxygen minimum began to diminish in early October and totally disappeared in November, under conditions of weakening stratification and intensifying mixing.

In conclusion, goodness of fit estimates showed an excellent performance of W2 in Rappbode Reservoir with very precise predictions for the physical variables (water level and temperature), high accuracy for chemical variables (oxygen and nutrients), and also good accuracy for biological state variables (diatoms and *P. rubescens*). These high model skills enable us to use the model for a process-oriented systems analysis.

3.2. Sensitivity analysis and model robustness

The analysis of parameter sensitivity identified a few highly sensitive parameters with respect to the minimum oxygen concentration within the MOM, which are either involved in diatom dynamics, sediment oxygen demand or *P. rubescens* dynamics (see Table 1). Interestingly, these most sensitive parameters were not centered around a specific state variable (e.g. *P. rubescence*) but refer to pelagic as well as benthic components indicating that both pelagic and benthic processes can have a strong effect on the minimum oxygen concentration of the MOM.

The phenomenon of MOM appeared highly robust against the parameterization as perturbations of the parameters never produced oxygen dynamics without a MOM. The minimum concentration, the depth location is varying slightly with parameter changes (see SI

for a detailed description) but the patterns of vertical DO gradients remained similar. The minimum oxygen concentration from the calibrated model, for example, was at 5 mg L^{-1} and in all simulations with perturbed parameters this value remained in the range of 4.3 to 5.7 mg L^{-1} (Figure S6).

3.3. Mechanistic understanding of MOM formation

The separate effect of pelagic (*P. rubescens* and diatoms) and benthic processes (SOD) on the metalimnetic DO concentration is illustrated in Figure 8. In the absence of *P. rubescens* (scenario B), the diatom concentration in the metalimnion (depth of 10 m) during the summer (day 180 to 250) increased slightly from 1.26 mg L^{-1} in the reference scenario (A) to 1.83 mg L^{-1}. Notably, the MOM was more pronounced in scenario B, with an average DO concentration of 6.28 mg L^{-1} in the autumn MOM layer (taken as the water layer between 10 to 20 m and from day 240 to 300), which was lower than the 6.75 mg L^{-1} in the reference simulation.

In scenario C, the simulation without diatoms, *P. rubescens* bloomed one month earlier (at the end of June) than in the reference simulation (at the end of July). The metalimnetic algal concentration reached 20 µg L^{-1} in scenario C, which was twice as high as in the reference simulation. This, in turn, produced a local metalimnetic oxygen maximum in early summer that reached a concentration up to 14 mg L^{-1}. Although a weak MOM was still present in scenario C from day 250 onwards, the average DO concentration in the autumn MOM layer was 8.31 mg L^{-1}, which was much higher than in the reference simulation (6.75 mg L^{-1}). Additionally, the hypolimnetic DO concentrations were higher in scenario C than in

the reference simulation. Scenario C demonstrates that the presence of *P. rubescens* postpones and weakens the MOM because during the growth phase a net oxygen production occurs within the metalimnion and no oxygen consumption from diatom-derived biomass (reference scenario) is taking place.

The most remarkable result from scenario D was that the MOM was still present despite the absence of both diatoms and *P. rubescens.* With essentially no organic matter production in the water column, the oxygen in the metalimnion in this scenario is consumed solely by the sediment resulting in a MOM with an average DO concentration of 8.52 mg L^{-1}. Oxygen depletion from metalimnetic sediments is higher than that from the deeper hypolimnetic sediments because of higher temperature at this depth compared to deeper layers. This conclusion is further confirmed by the results in scenario E, in which only the SOD was turned off while the algae were still present. This scenario clearly showed that only the activities from the two algal groups cannot trigger the MOM.

Finally, the MOM also disappeared completely in our control scenario F, i.e. when all the pelagic processes were removed and SOD was set to 0. In this case, the DO distribution in the water column was solely driven by temperature-dependent oxygen solubility at the different depths and atmospheric equilibrium within the epilimnion.

In order to quantify the contributions from the different processes at play in the formation of the MOM, we extracted the oxygen production rates from photosynthesis, and the consumption rates from organic matter decay and sediment oxygen demand out of the reference simulation. Oxygen production by photosynthesis reached 0.2 mg $L^{-1} \cdot day^{-1}$ in the surface layer during the spring diatom bloom, which began at the time of stratification onset

around day 100 (Figure 9A). After the spring bloom, diatoms continued to produce oxygen in the metalimnion at a lower rate. Between day 150 and 200, *P. rubescens* replaced diatoms in the metalimnion. The oxygen production rate was then lower than in spring and reached values around 0.1 mg $L^{-1} \cdot day^{-1}$. The DO consumption through decomposition of pelagic organic material derived from dead algae was high in spring in the surface layers (day 100-160, Figure 9B) with maximum values of 0.08 mg $L^{-1} \cdot day^{-1}$. Afterwards, DO consumption remained relatively high in the metalimnion for another 2 months. After day 220, DO consumption by organic matter decreased in the metalimnion, with an average rate of 0.009 mg $L^{-1} \cdot day^{-1}$ in autumn within the MOM layer. The sediment consumed a large amount of oxygen in the bottom layers (Figure 9C) due to the high ratio of sediment area to water volume. Given the strong temperature dependence of sediment oxygen consumption rate, sediment oxygen consumption was also high in the warmer layers of the epilimnion and metalimnion (Figure 9C). The average oxygen consumption rate in the autumn MOM layer, caused by SOD, was 0.015 mg $L^{-1} \cdot day^{-1}$. Taken together all the different oxygen production and consumption terms (Figure 9D), about 60% of the total simulated consumption rate in the autumn MOM layer (i.e. 0.024 mg $L^{-1} \cdot day^{-1}$) originated from benthic processes, while the remaining 40% originated from pelagic mineralization of dead algal biomass. In conclusion, the MOM is formed by both pelagic and benthic DO depletion. *P. rubescens* delivers large parts of the pelagic organic matter that fuels pelagic DO consumption, but it also produces oxygen during the growth phase and therefore effectively postpones the MOM formation.

4. Discussion

In this study, we used a well-developed water quality model to identify and analyze the drivers of MOM formation. On the one hand, our research confirms the previous conclusion from Wentzky et al. (2019) that the occurrence of *P. rubescens* delivers an important contribution for the formation of the MOM. On the other hand, this study also shows that the process chain is more complex and SOD also significantly contributes to the phenomenon. Our study is innovative because we employed an ecosystem model not only to reproduce observations and quantitative patterns, but also to identify and quantify processes and test hypotheses in a series of simulation experiments. Our model system combines the major physical (e.g. vertical transport and thermodynamics), biogeochemical (e.g. nutrient and oxygen dynamics), and ecological (e.g. algal community dynamics, resource limitation) features of this complex ecosystem.

The simulation results were in good agreement with measurements for all variables and the RMSE for the water temperature was lower than that obtained in other recent studies (Chong et al. 2018; Lee et al. 2018; Park et al. 2018). Based on a meta-analysis of the performance of different water quality models by Arhonditsis and Brett (2004), the simulation accuracy of water temperature in this study can be regarded as top level. Furthermore, the model accurately reproduced the dynamics of nutrients, two main algal groups in the reservoir (diatoms and *P. rubescens)* and dissolved oxygen, particularly the temporal and spatial extent of the MOM (see Figure 3-7). The R^2 of 0.84 for oxygen is much higher than the median value of 0.70 calculated from 569 oxygen modelling studies shown in Arhonditsis and Brett (2004).

Using a 1D physical-biological coupled model, Joehnk and Umlauf (2001) and Antonopoulos and Gianniou (2003) also captured the MOM in Lake Ammer and Lake Vegoritis, respectively. However, these models only considered total chlorophyll-a rather than the dynamics of different phytoplankton groups. As suggested by Joehnk and Umlauf (2001), merely simulating the chlorophyll-a is too general and accounting for specific algal properties can improve the accuracy of model simulations. Our work substantiates this statement as the ecological features of the different algal groups in our model play an important role in the MOM formation. However, although our model is far more detailed than previous approaches, we were also forced to apply simplications in terms of process formulations and state variables. Zooplankton grazing, for example, is only indirectly represented by algae mortality and bacterial respiration is integrated into degradation of organic matter. The diverse phytoplankton community is reduced to two functional groups (diatoms, *P. rubescens*), which largely represent the photoautotrophic organisms but not mixotrophs, which occur during late summer in Rappbode Reservoir. To the best of our knowledge, however, this work is the first modelling research which systematically elucidates the mechanisms that trigger MOMs in inland waters in a process chain including biogeochemical and ecological dynamics.

A detailed evaluation of the model with respect to sensitivity and robostness corroborated with the findings from our simulation experiments in the respect that parameters for algal dynamics as well as sediment-related parameters were highly sensitive. This implies that both pelagic and benthic processes have a large influence on the MOM. Our model findings were also robust against the parameterization. The phenomenon of a MOM was formed under all parameter perturbations and can be classified as a very robust feature of the

508 Rappbode Reservoir model. We interpret this outcome as an indicator that our conclusions
509 are valid over a broad range of parametter values.
510
511 **Processes driving formation of a metalimnetic oxygen minimum**
512
513 Our results identify a chain of events leading to the formation of the MOM that is more
514 complex than the mechanism described in Wentzky et al. (2019). Comparing scenario A and
515 B (see Figure 8) showed that diatoms also contributed to the formation of MOM since
516 sinking organic matter, originating from dead diatoms, consumed DO in the metalimnion. In
517 the reference simulation, however, this DO consumption was not visible because the growing
518 *P. rubescens* replaced the dying diatoms and the DO that *P. rubescens* produced was utilized
519 to break down the diatom biomass. Therefore, DO remained rather constant during this time
520 although the turnover was high. In the absence of diatoms in scenario C, the earlier onset of *P.*
521 *rubescens* therefore triggered a metalimnetic oxygen maximum in late spring and delayed and
522 decreased MOM formation, although decomposition of organic material from dead *P.*
523 *rubescens* ultimately transformed the metalimnetic oxygen maximum into a minimum.
524 Moreover, when *P. rubescens* was excluded from the simulation in scenario B, the MOM
525 formed earlier and attained a lower DO concentration because organic matter degradation
526 from diatoms and SOD consumed oxygen from day 150 onwards. In fact, the occurrence of *P.*
527 *rubescens* delayed and slightly weakened the MOM, although its biomass ultimately induced
528 the MOM. Additonally, a weak but clear oxygen minimum still formed in the metalimnion in
529 scenario D, which did not contain any algae (Figure 8) but SOD as the sole DO sink. In order

to assure that the value of SOD in our model is within a reasonable empirical range we extracted SOD values from other water bodies from literature (SI Table S2). It turned out that our value of 3 gO_2 m^{-2} d^{-1} is a typical value that can also be found in other water bodies. This indicates that benthic oxygen conspumtion can significantly influence metalimnetic oxygen dynamics in other lakes or reservoirs.

Shapiro (1960) identified three factors that might lead to the formation of a MOM: 1) inflow with low oxygen content; 2) in-situ biological and chemical processes; 3) sediment consumption. In Rappbode Reservoir, the first factor could be excluded since oxygen from the inflows was always saturated. Also, the MOM was captured at depths between 11 m and 13 m in front of the dam. As illustrated in Figure S7, during the period of the MOM formation, the inflows were much warmer than water at 11 m depth, even during nocturnal cooling events in exceptionally cold summer nights. Only in mid-October, i.e. at the time of MOM erosion, inflow temperatures approached metalimnetic temperatures. Also high loads of sediments as an alternative process for deep inflow intrusions can be ruled out because almost all of the sediments from the inflow are efficiently retained in the upstream pre-dams. Additionally, the total inflow discharge during the occurrence of the MOM (i.e. from day 240 to 300) was very low (always lower than 0.5 m^3 s^{-1}, see Figure S8). In conclusion, any influence of inflows on MOM formation can be ruled out. The remaining two factors from Shapiro (1960), in situ biological/chemical processes and SOD, appeared to contribute to the MOM formation in Rappbode Reservoir as shown by our scenario analysis.

We further extracted and compared the simulated oxygen profiles at shallower sections in the reservoir, at the same time of 2016 (10^{th} September) as the measurements in 2015 from

Wentzky et al. (2019) (see Figure S9). Although we do not have the corresponding measured oxygen profiles in 2016, based on our knowledge of the reservoir, the principal oxygen distribution patterns were similar in 2015 and 2016 and the oxygen patterns should be comparable. We found that horizontal variablility of the simulated MOM in 2016 was a little larger than that of the measurements in 2015 (see their Fig. 3). This may be a sign that our model did not completely capture the contribution of benthic and pelagic oxygen depletion along the longitudinal axis. The morphometry of Rappbode Reservoir is characterised by steep slopes that do not allow the formation of sustained sediment layers at many places. We therefore speculate that the SOD in the canyon-shaped, upstream parts is lower than that in the central basin, where plankton growth and sedimentation of organic material is much higher. Hence, we may have slightly overestimated the contribution of SOD to the formation of the MOM at these upstream sites. However, this should not change our conclusion that the SOD plays an important role in the MOM development.

Besides these biogeochemical drivers, the physical environment is decisive for the persistence of a MOM. The metalimnion is a region with low vertical mixing due to strong density gradients and this mixing refuge prevents the MOM from being refilled with oxygen from above or below (Dong et al. 2019). This low mixing refuge is clearly evident in the Rappbode Reservoir and a commmon feature of stably stratified lakes and reservoirs (Boehrer and Schultze 2008).

The role of temperature

574 We believe that the oxygen uptake by the sediment contributes to the MOM in the
575 Rappbode Reservoir. Water temperature alone can change the SOD rate by a factor of 10
576 within the range of 4-30 °C (Pace and Prairie 2005), which is in accordance with our
577 calibrated SOD temperature-rate multipliers (see Table 1). The sediment oxygen consumption
578 rate is therefore highly sensitive to water temperature (Terry et al. 2017). In Rappbode
579 Reservoir, water temperature below 20 m depth is below 6 °C the whole year round (Figure
580 S10). The low water temperatures in these layers decrease oxygen consumption from the
581 sediment. In contrast, the temperature in the upper 15 m (e.g. metalimnion and epilimnion) is
582 always above 10 °C in summer, which leads to a relatively high sediment oxygen demand. In
583 the epilimnion, atmospheric exchange can offset the sediment uptake.In the metalimnion (i.e.
584 10 m to 15 m depth), however, the low vertical diffusivity caused by intense stratification
585 strongly inhibits any flux of oxygen from above or below. Therefore, the high SOD rate,
586 which results from the warm temperature combined with the disconnection from the
587 atmosphere, is a significant factor causing the MOM in the reservoir.

588 Higher temperatures also significantly enhance algal biomass decay rates (Conover et al.
589 2016). England et al. (2015) concluded that, compared to the beginning of the 21st century,
590 the global mean temperature at the end of the century will increase by nearly 5 °C under high
591 greenhouse gas emissions. Also, surface water temperatures have increased globally by
592 0.34 °C decade^{-1} in recent decades (O'Reilly and Sharma 2015). Possibly, higher water
593 temperatures under strong climate warming may increase the MOM in future. In temperate
594 climates, this trend is further enhanced by an increasing stratification duration (Fang and
595 Stefan 2009; Radbourne et al. 2019; Shatwell et al. 2019). Therefore, further modelling

scenarios should focus on how to optimize management practices (e.g. artificial aeration, different withdrawal depths) to mitigate the negative influence caused by the increase in air temperatures.

The advanced water quality model in this study systematically explained the ecological processes related to the MOM formation in Rappbode Reservoir. We extended the findings of Wentzky et al. (2019) by showing that not only pelagic, but also benthic processes contribute to MOM formation, where the strong temperature and density gradients in the metalimnion play a decisive role. Since MOMs are widespread in stratified lakes and reservoirs, our model may be transferred to other systems to identify the drivers responsible for MOMs in different case studies. A valuable next step would therefore be an application of this model in a multi-lake comparison to better understand the mechanisms behind MOM development at a large scale.

5. Conclusions

In this study, we used a well-established water quality model (CE-QUAL-W2) to illustrate the mechanism behind the formation of metalimnetic oxygen minima (MOM) in Rappbode Reservoir. The results showed that our model performed well in reproducing the physical (e.g. water level and water temperature), biogeochemical (e.g. nutrient and oxygen dynamics) and ecological (e.g. algal community dynamics) features of the reservoir, particularly the spatial and temporal extent of the MOM. Through a scenario analysis we found that growth of the cyanobacterium *Planktothrix rubescens* in the metalimnion

postponed and weakened the MOM through photosynthesis, although the decomposition of its biomass ultimately induced the MOM. Moreover, the results showed that not only pelagic processes, but also benthic processes (e.g. sediment oxygen demand) contributed to the formation of the MOM. Besides these biogeochemical drivers, the physical environment was demonstrated as a determinant for the persistence of a MOM. The high density gradient in the thermocline restricted downward transport of oxygen from surface waters, yet the higher temperatures in the metalimnion relative to the hypolimnion caused locally increased oxygen consumption rates from the sediment and decaying organic matter which contributed to the formation of the MOM. Since the global warming trend is supposed to increase the MOM in future, it is recommended in the further modelling scenarios to elucidate how to optimize the reservoir operation strategies to adapt the negative influence caused by the climate change.

Acknowledgements

The authors are grateful to the Rappbode Reservoir authority (Talsperrenbetrieb Sachsen-Anhalt), the Fernwasserversorgung Elbaue-Ostharz GmbH and German Weather Service (DWD) for provision of the hydrological and meteorological data. We also thank Philipp Keller for preparing the bathymetric map. The authors acknowledge financial support from the China Scholarship Council (CSC), the newMOM-project funded by the German Science Foundation under grant RI 2040/4-1, the National Natural Science Foundation of China (grant 31670711) as well as the ERA4CS-Project "WateXr" funded under grant 01LS1713A from the German Federal Ministry of Education and Research. Finally, we thank two anonymous reviewers for their constructive comments to an earlier version of this manuscript.

References

Antonopoulos, V. Z. & S. K. Gianniou, 2003. Simulation of water temperature and dissolved oxygen distribution in Lake Vegoritis, Greece. Ecological Modelling 160(1-2):39-53.

Arhonditsis, G. B. & M. T. Brett, 2004. Evaluation of the current state of mechanistic aquatic biogeochemical modeling. Mar Ecol Prog Ser 271:13-26 doi:http://dx.doi.org/10.3354/meps271013.

Boehrer, B. & M. Schultze, 2008. Stratification of lakes. Rev Geophy 46:RG 2005 doi:10.1029/2006RG000210.

Bolton, D., 1980. The computation of equivalent potential temperature. Mon Weather Rev 108(7):1046-1053.

Brito, D., T. B. Ramos, M. C. Gonçalves, M. Morais & R. Neves, 2018. Integrated modelling for water quality management in a eutrophic reservoir in south-eastern Portugal. Environmental Earth Sciences 77(2):40.

Carraro, E., N. Guyennon, D. Hamilton, L. Valsecchi, E. C. Manfredi, G. Viviano, F. Salerno, G. Tartari & D. Copetti, 2012. Coupling high-resolution measurements to a three-dimensional lake model to assess the spatial and temporal dynamics of the cyanobacterium Planktothrix rubescens in a medium-sized lake Hydrobiologia. Springer, 77-95.

Chang, C. H., L. Y. Cai, T. F. Lin, C. L. Chung, L. van der Linden & M. Burch, 2015. Assessment of the Impacts of Climate Change on the Water Quality of a Small Deep Reservoir in a Humid-Subtropical Climatic Region. Water 7(4):1687-1711 doi:10.3390/w7041687.

Chong, S., C. Park, K. Lee & K.-G. An, 2018. Modeling Summer Hypoxia Spatial Distribution and Fish Habitat Volume in Artificial Estuarine Waterway. Water 10(11):1695.

Chuo, M., J. Ma, D. Liu & Z. Yang, 2019. Effects of the impounding process during the flood season on algal blooms in Xiangxi Bay in the Three Gorges Reservoir, China. Ecological Modelling 392:236-249 doi:http://dx.doi.org/10.1016/j.ecolmodel.2018.11.017.

Cole, T. M. & S. A. Wells, 2006. CE-QUAL-W2: A two-dimensional, laterally averaged, hydrodynamic and water quality model, version 3.5.

Conover, J., L. A. Green & C. S. Thornber, 2016. Biomass decay rates and tissue nutrient loss in bloom and non-bloom-forming macroalgal species. Estuar Coast Shelf Sci 178:58-64.

Dong, F., C. Mi, M. Hupfer, K. E. Lindenschmidt, W. Peng, X. Liu & K. Rinke, 2019. Assessing vertical diffusion in a stratified lake using a 3D hydrodynamic model. Hydrological Processes.

Elliott, J. A., 2012. Is the future blue-green? A review of the current model predictions of how climate change could affect pelagic freshwater cyanobacteria. Water research 46(5):1364-1371.

England, M. H., J. B. Kajtar & N. Maher, 2015. Robust warming projections despite the recent hiatus. Nature Climate Change 5(5):394-396 doi:http://dx.doi.org/10.1038/nclimate2575.

Fang, X. & H. G. Stefan, 2009. Simulations of climate effects on water temperature, dissolved oxygen, and ice and snow covers in lakes of the contiguous United States under past and future climate scenarios. Limnology and Oceanography 54:2359-2370.

Fenocchi, A., M. Rogora, G. Morabito, A. Marchetto, S. Sibilla & C. Dresti, 2019. Applicability of a one-dimensional coupled ecological-hydrodynamic numerical model to future projections in a very deep large lake (Lake Maggiore, Northern Italy/Southern Switzerland). Ecological Modelling 392:38-51.

Foley, B., I. D. Jones, S. C. Maberly & B. Rippey, 2012. Long‐term changes in oxygen depletion in a small temperate lake: effects of climate change and eutrophication. Freshwater Biology 57(2):278-289.

Friese, K., M. Schultze, B. Boehrer, O. Büttner, P. Herzsprung, M. Koschorreck, B. Kuehn, H. Rönicke, K. Wendt‐

685 Potthoff & U. Wollschläger, 2014. Ecological response of two hydro‐morphological similar pre‐dams
686 to contrasting land‐use in the Rappbode reservoir system (Germany). International Review of
687 Hydrobiology 99(5):335-349.
688 Hamilton, D. P. & S. G. Schladow, 1997. Prediction of water quality in lakes and reservoirs. Part I—Model
689 description. Ecological Modelling 96(1-3):91-110.
690 Horppila, J., T. Malinen, L. Nurminen, P. Tallberg & M. Vinni, 2000. A metalimnetic oxygen minimum indirectly
691 contributing to the low biomass of cladocerans in Lake Hiidenvesi–a diurnal study on the refuge effect.
692 Hydrobiologia 436(1-3):81-90.
693 Hupfer, M. & J. Lewandowski, 2008. Oxygen Controls the Phosphorus Release from Lake Sediments – a
694 Long-Lasting Paradigm in Limnology. International Review of Hydrobiology 93(4‐5):415-432
695 doi:doi:10.1002/iroh.200711054.
696 Joehnk, K. D. & L. Umlauf, 2001. Modelling the metalimnetic oxygen minimum in a medium sized alpine lake.
697 Ecological Modelling 136(1):67-80 doi:10.1016/s0304-3800(00)00381-1.
698 Kang, M., S. Peng, Y. Tian & H. Zhang, 2018. Effects of dissolved oxygen and nutrient loading on phosphorus
699 fluxes at the sediment–water interface in the Hai River Estuary, China. Mar Pollut Bull 130:132-139.
700 Knoll, L. B., C. E. Williamson, R. M. Pilla, T. H. Leach, J. A. Brentrup & T. J. Fisher, 2018. Browning-related oxygen
701 depletion in an oligotrophic lake. Inland Waters 8(3):255-263.
702 Kobler, U. G., A. Wüest & M. Schmid, 2018. Combined effects of pumped-storage operation and climate change
703 on thermal structure and water quality. Climatic Change doi:10.1007/s10584-018-2340-x.
704 Kreling, J., J. Bravidor, C. Engelhardt, M. Hupfer, M. Koschorreck & A. Lorke, 2017. The importance of physical
705 transport and oxygen consumption for the development of a metalimnetic oxygen minimum in a lake.
706 Limnology and Oceanography 62(1):348-363 doi:http://dx.doi.org/10.1002/lno.10430.
707 Ladwig, R., E. Furusato, G. Kirillin, R. Hinkelmann & M. Hupfer, 2018. Climate Change Demands Adaptive
708 Management of Urban Lakes: Model-Based Assessment of Management Scenarios for Lake Tegel
709 (Berlin, Germany). Water 10(2) doi:10.3390/w10020186.
710 Lee, R., T. Biggs & X. Fang, 2018. Thermal and Hydrodynamic Changes under a Warmer Climate in a Variably
711 Stratified Hypereutrophic Reservoir. Water 10(9):1284.
712 Liljendahl-Nurminen, A., J. Horppila & W. Lampert, 2008. Physiological and visual refuges in a metalimnion: an
713 experimental study of effects of clay turbidity and an oxygen minimum on fish predation. Freshwater
714 Biology 53(5):945-951.
715 Livingstone, D. M. & D. M. Imboden, 1996. The prediction of hypolimnetic oxygen profiles: a plea for a
716 deductive approach. Canadian Journal of Fisheries and Aquatic Sciences 53(4):924-932.
717 McClure, R. P., K. D. Hamre, B. Niederlehner, Z. W. Munger, S. Chen, M. E. Lofton, M. E. Schreiber & C. C. Carey,
718 2018. Metalimnetic oxygen minima alter the vertical profiles of carbon dioxide and methane in a
719 managed freshwater reservoir. Science of The Total Environment 636:610-620.
720 Mi, C., M. A. Frassl, B. Boehrer & K. Rinke, 2018. Episodic wind events induce persistent shifts in the thermal
721 stratification of a reservoir (Rappbode Reservoir, Germany). International Review of Hydrobiology
722 103:71-82 doi:http://dx.doi.org/10.1002/iroh.201701916.
723 Mi, C., A. Sadeghian, K.-E. Lindenschmidt & K. Rinke, 2019. Variable withdrawal elevations as a management
724 tool to counter the effects of climate warming in Germany's largest drinking water reservoir.
725 Environmental Sciences Europe 31(1):19 doi:https://doi.org/10.1186/s12302-019-0202-4.
726 Mooij, W. M., D. Trolle, E. Jeppesen, G. Arhonditsis, P. V. Belolipetsky, D. B. R. Chitamwebwa, A. G.
727 Degermendzhy, D. L. DeAngelis, L. N. De Senerpont Domis, A. S. Downing, J. A. Elliott, C. R. Fragoso, U.
728 Gaedke, S. N. Genova, R. D. Gulati, L. Håkanson, D. P. Hamilton, M. R. Hipsey, J. 't Hoen, S. Hülsmann, F.

H. Los, V. Makler-Pick, T. Petzoldt, I. G. Prokopkin, K. Rinke, S. A. Schep, K. Tominaga, A. A. Van Dam, E. H. Van Nes, S. A. Wells & J. H. Janse, 2010. Challenges and opportunities for integrating lake ecosystem modelling approaches. Aquat Ecol 44(3):633-667 doi:10.1007/s10452-010-9339-3.

Müller, B., L. D. Bryant, A. Matzinger & A. Wüest, 2012. Hypolimnetic oxygen depletion in eutrophic lakes. Environmental Science & Technology 46(18):9964-9971 doi:https://doi.org/10.1021/es301422r.

Nix, J., 1981. Contribution of hypolimnetic water on metalimnetic dissolved oxygen minima in a reservoir. Water Resources Research 17(2):329-332 doi:doi:10.1029/WR017i002p00329.

O'Reilly, C. M. & S. Sharma, 2015. Rapid and highly variable warming of lake surface waters around the globe. Geophysical Research Letters 42:10773-10781 doi:10.1002/.

Pace, M. L. & Y. T. Prairie, 2005. Respiration in lakes. Respiration in Aquatic Ecosystems 1:103-122.

Park, H., S. Chung, E. Cho & K. Lim, 2018. Impact of climate change on the persistent turbidity issue of a large dam reservoir in the temperate monsoon region. Climatic Change:1-14 doi:http://dx.doi.org/10.1007/s10584-018-2322-z.

Posch, T., O. Koster, M. M. Salcher & J. Pernthaler, 2012. Harmful filamentous cyanobacteria favoured by reduced water turnover with lake warming. Nature Climate Change 2(11):809-813 doi:http://dx.doi.org/10.1038/nclimate1581.

Radbourne, A. D., J. A. Elliott, S. C. Maberly, D. B. Ryves & N. J. Anderson, 2019. The impacts of changing nutrient load and climate on a deep, eutrophic, monomictic lake. Freshwater Biology.

Rangel-Peraza, J. G., J. De Anda, F. A. González-Farías & M. Rode, 2016. Sensitivity and uncertainty analysis on water quality modelling of Aguamilpa reservoir. J Limnol.

Rhodes, J., H. Hetzenauer, M. A. Frassl, K.-O. Rothhaupt & K. Rinke, 2017. Long-term development of hypolimnetic oxygen depletion rates in the large Lake Constance. Ambio 46(5):554-565 doi:10.1007/s13280-017-0896-8.

Rice, J. A., J. S. Thompson, J. A. Sykes & C. T. Waters, The role of metalimnetic hypoxia in striped bass summer kills: consequences and management implications. In: Am Fish Soc Symp, 2013. vol 80. p 000-000.

Rinke, K., B. Kuehn, S. Bocaniov, K. Wendt-Potthoff, O. Buttner, J. Tittel, M. Schultze, P. Herzsprung, H. Ronicke, K. Rink, K. Rinke, M. Dietze, M. Matthes, L. Paul & K. Friese, 2013. Reservoirs as sentinels of catchments: the Rappbode Reservoir Observatory (Harz Mountains, Germany). Environmental Earth Sciences 69(2):523-536 doi:http://dx.doi.org/10.1007/s12665-013-2464-2.

Rogora, M., F. Buzzi, C. Dresti, B. Leoni, F. Lepori, R. Mosello, M. Patelli & N. Salmaso, 2018. Climatic effects on vertical mixing and deep-water oxygen content in the subalpine lakes in Italy. Hydrobiologia:1-18.

Sadeghian, A., S. C. Chapra, J. Hudson, H. Wheater & K.-E. Lindenschmidt, 2018. Improving in-lake water quality modeling using variable chlorophyll a/algal biomass ratios. Environmental Modelling & Software 101:73-85 doi:http://dx.doi.org/10.1016/j.envsoft.2017.12.009.

Shapiro, J., 1960. THE CAUSE OF A METALIMNETIC MINIMUM OF DISSOLVED OXYGEN 1. Limnology and Oceanography 5(2):216-227.

Shatwell, T., W. Thiery & G. Kirillin, 2019. Future projections of temperature and mixing regime of European temperate lakes. Hydrology and Earth System Sciences 23(3):1533-1551 doi:http://dx.doi.org/10.5194/hess-23-1533-2019.

Terry, J. A., A. Sadeghian & K.-E. Lindenschmidt, 2017. Modelling dissolved oxygen/sediment oxygen demand under ice in a shallow eutrophic prairie reservoir. Water 9(2):131.

Walsby, A. E. & F. Jüttner, 2006. The uptake of amino acids by the cyanobacterium Planktothrix rubescens is stimulated by light at low irradiances. Fems Microbiol Ecol 58(1):14-22.

Wang, L. K., D. Vielkind & M. H. Wang, 1978. Mathematical models of dissolved oxygen concentration in fresh

773 water. Ecological Modelling 5(2):115-123.
774 Weber, M., K. Rinke, M. Hipsey & B. Boehrer, 2017. Optimizing withdrawal from drinking water reservoirs to
775 reduce downstream temperature pollution and reservoir hypoxia. Journal of Environmental
776 Management 197:96-105 doi:http://dx.doi.org/10.1016/j.jenvman.2017.03.020.
777 Wentzky, V. C., M. A. Frassl, K. Rinke & B. Boehrer, 2019. Metalimnetic oxygen minimum and the presence of
778 Planktothrix rubescens in a low-nutrient drinking water reservoir. Water Research(148):208-218.
779 Wentzky, V. C., J. Tittel, C. G. Jäger & K. Rinke, 2018. Mechanisms preventing a decrease in phytoplankton
780 biomass after phosphorus reductions in a German drinking water reservoir—results from more than
781 50 years of observation. Freshwater biology 63(9):1063-1076
782 doi:http://dx.doi.org/10.1111/fwb.13116.
783 Wetzel, R. G., 2001. Limnology,3rd ed. Academic Press.
784 Zhang, Y., Z. Wu, M. Liu, J. He, K. Shi, Y. Zhou, M. Wang & X. Liu, 2015. Dissolved oxygen stratification and
785 response to thermal structure and long-term climate change in a large and deep subtropical reservoir
786 (Lake Qiandaohu, China). Water Research 75:249-258.
787

788

Tables

Table 1: Model parameter list for the Rappbode Reservoir

Parameter	Description	Calibrated Value	SSC
WSC*	Wind sheltering coefficient	0.9	----
SHADE	Shading coefficient	1	----
EXH20	Extinction coefficient for algal-free water (m^{-1})	0.45	----
AG #1*	Algal growth rate for P-rub (day^{-1})	0.55	-1.3
AG #2*	Algal growth rate for diatoms (day^{-1})	1.5	-0.2
AR#1	Algal dark respiration rate for P-rub (day^{-1})	0.02	-1.1
AR#2	Algal dark respiration rate for diatoms (day^{-1})	0.05	-0.4
AE#1	Algal excretion rate for P-rub (day^{-1})	0.01	1.6
AE#2	Algal excretion rate for diatoms (day^{-1})	0.05	-0.2
AM#1	Algal mortality rate for P-rub (day^{-1})	0.005	-0.8
AM#2	Algal mortality rate for diatoms (day^{-1})	0.05	0.8
AS#1	Algal settling rate for P-rub (day^{-1})	0.001	-0.9
AS#2	Algal settling rate for diatoms (day^{-1})	0.05	0.5
AHSP#1	Algal half-saturation for phosphorus limited growth for P-rub ($g\ m^{-3}$)	0.002	1.2
AHSP#2	Algal half-saturation for phosphorus limited growth for diatoms ($g\ m^{-3}$)	0.002	-0.1
AHSN#1	Algal half-saturation for nitrogen limited growth for P-rub ($g\ m^{-3}$)	0.005	0.0
AHSN#2	Algal half-saturation for nitrogen limited growth for diatoms ($g\ m^{-3}$)	0.1	0.0
AHSSI#1	Algal half-saturation for silica limited growth for P-rub ($g\ m^{-3}$)	0	---
AHSSI#2	Algal half-saturation for silica limited growth for diatom ($g\ m^{-3}$)	0.1	0.0

Parameters	Description	Calibrated Value	SSC
ASAT#1*	Light saturation intensity at maximum photosynthetic rate for P-rub (W m^{-2})	8	0.2
ASAT#2*	Light saturation intensity at maximum photosynthetic rate for diatoms (W m^{-2})	35	0.2
AT1#1	Lower temperature for P-rub growth (^{o}C)	5	---
AT1#2	Lower temperature for diatoms growth (^{o}C)	0	---
AT2#1	Lower temperature for maximum P-rub growth (^{o}C)	10	0.1
AT2#2	Lower temperature for maximum diatoms growth (^{o}C)	11	0.8
AT3#1	Upper temperature for maximum P-rub growth (^{o}C)	14	-0.6
AT3#2	Upper temperature for maximum diatoms growth (^{o}C)	15	0.1
AT4#1	Upper temperature for P-rub growth (^{o}C)	18	-0.4
AT4#2	Upper temperature for diatoms growth (^{o}C)	30	0.0
ACHLA#1	Ratio between P-rub biomass and chlorophyll a in terms of mg algae/µg chl a	0.18	0.0
ACHLA#2	Ratio between diatoms biomass and chlorophyll a in terms of mg algae/µg chl a	0.12	0.0
O2AG#1	Oxygen stoichiometry for P-rub primary production (mg O_2/mg algae organic matter)	1.1	-1.3
O2AG#2	Oxygen stoichiometry for diatoms primary production (mg O_2/mg algae organic matter)	1.4	1.9
O2AR#1	Oxygen stoichiometry for P-rub primary respiration (mg O_2/mg algae organic matter)	1.1	-0.1
O2AR#2	Oxygen stoichiometry for diatoms primary respiration (mg O_2/mg algae organic matter)	1.4	0.6
ORGP	Stoichiometric equivalent between organic matter and phosphorus	0.005	0.0
ORGN	Stoichiometric equivalent between organic matter and nitrogen	0.08	0.0

Parameters	Description	Calibrated Value	SSC
ORGC	Stoichiometric equivalent between organic matter and carbon	0.45	0.0
ORGSI	Stoichiometric equivalent between organic matter and silica	0.18	0.0
POMS	Particulate organic matter settling rate (m day^{-1})	0.5	0.0
PO4R	Sediment release rate of phosphorus, fraction of SOD	0.015	0.9
NH4R	Sediment release rate of ammonium, fraction of SOD	0.15	-0.3
NH4DK	Ammonium decay rate (day^{-1})	0.15	0.3
NO3DK	Nitrate decay rate (day^{-1})	0.05	0.2
DSIR	Dissolved silica sediment release rate, fraction of SOD	0.1	0.0
SOD	Maximum sediment oxygen demand ($gO_2\ m^{-2}\ day^{-1}$)	3	-1.4
SODT1	Lower temperature for SOD (^oC)	4	0.1
SODT2	Upper temperature for SOD (^oC)	30	0.8
SODK1	Fraction of SOD at lower temperature	0.1	0.0
SODK2	Fraction of SOD at upper temperature	0.99	---

* The parameter used for calibration

Table 2: Summary of the performance indicators for the W2 modeling of hydrodynamic and water quality variables, RMSE = root mean squared error, R^2 = coefficient of determination, NSE = Nash-Sutcliffe efficiency

Simulated Variables	**RMSE**	**R^2**	NSE
Water level (m)	0.03	0.99	0.99
Water temperature (°C)	0.45	0.99	0.99
NO_3 (mg/l)	0.14	0.69	-0.07
Silicate (mg/l)	0.29	0.84	0.57
Diatom (µg/L)	0.73	0.55	0.44
Planktothrix-rubescens (µg/L)	0.65	0.56	0.19
Oxygen (mg/l)	0.95	0.84	0.68

Figures

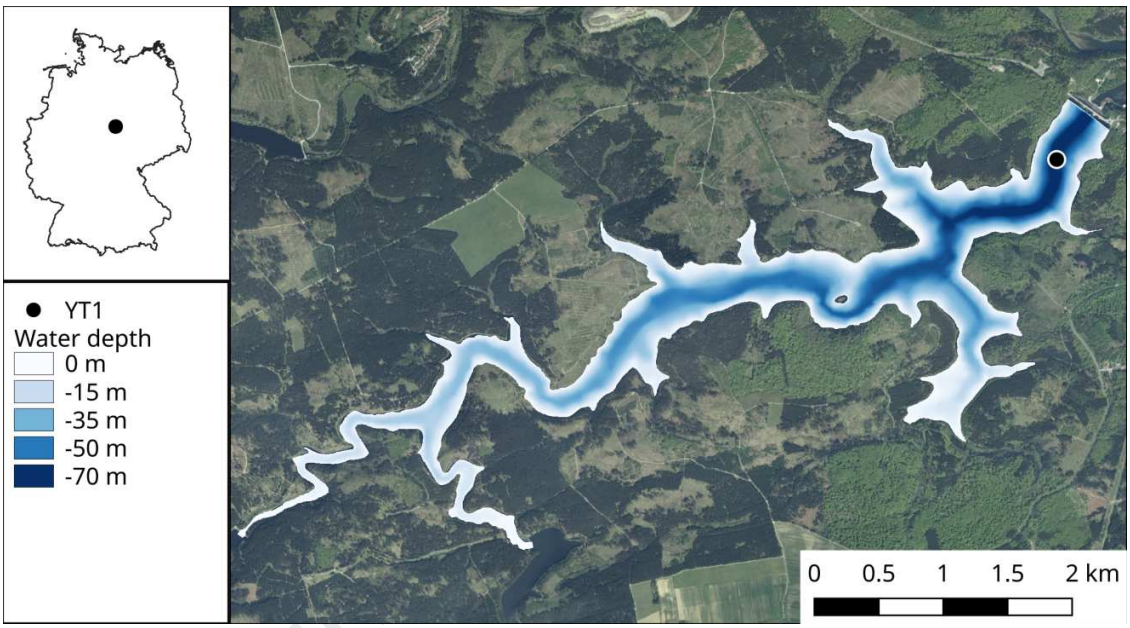

Figure 1. Map of Germany (top left). The black point indicates the location of Rappbode Reservoir. Bathymetric map of the Rappbode Reservoir (right). The black point shows the sampling location.

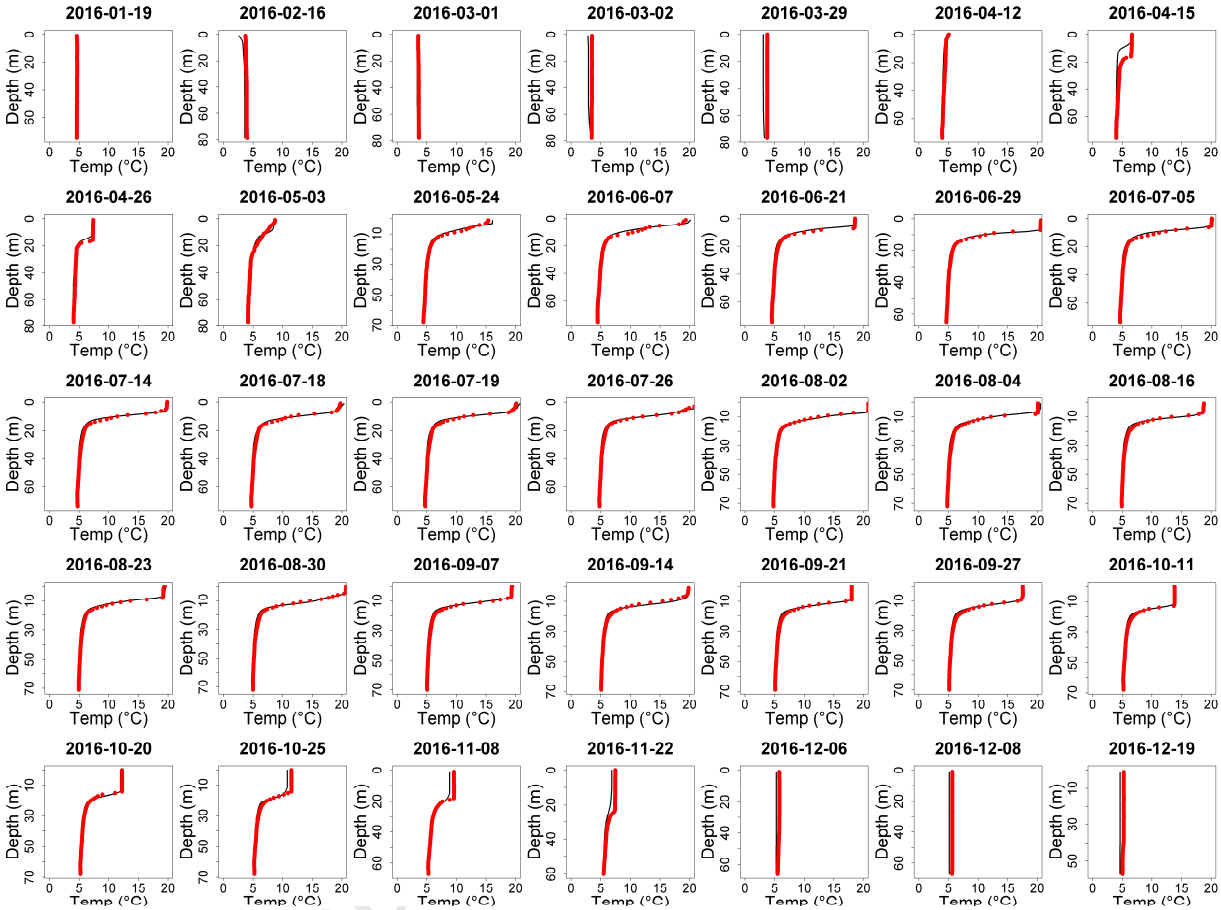

Figure 2. Comparison between simulation (black lines) and observation (red points) for water temperature for different dates in 2016.

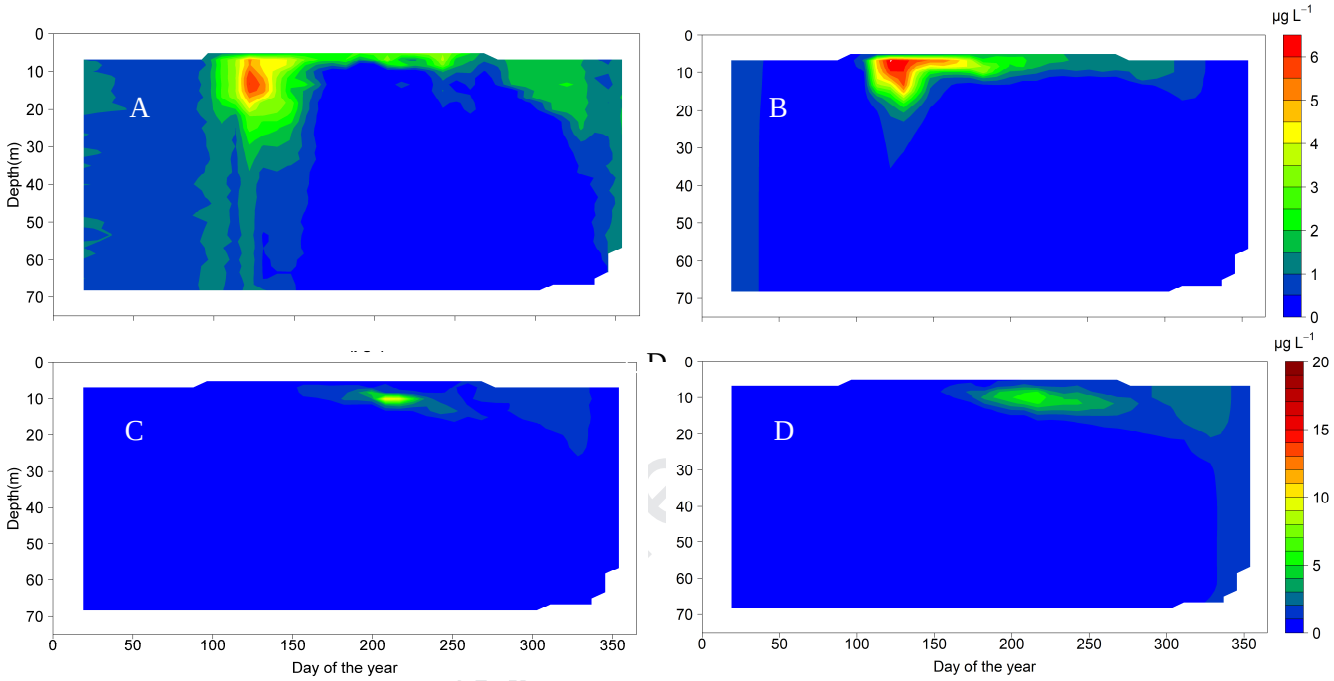

Figure 3. Comparison between observed (left) and simulated (right) algal concentrations in 2016 : (A and B) diatoms; (C and D) *P.rubescens*.

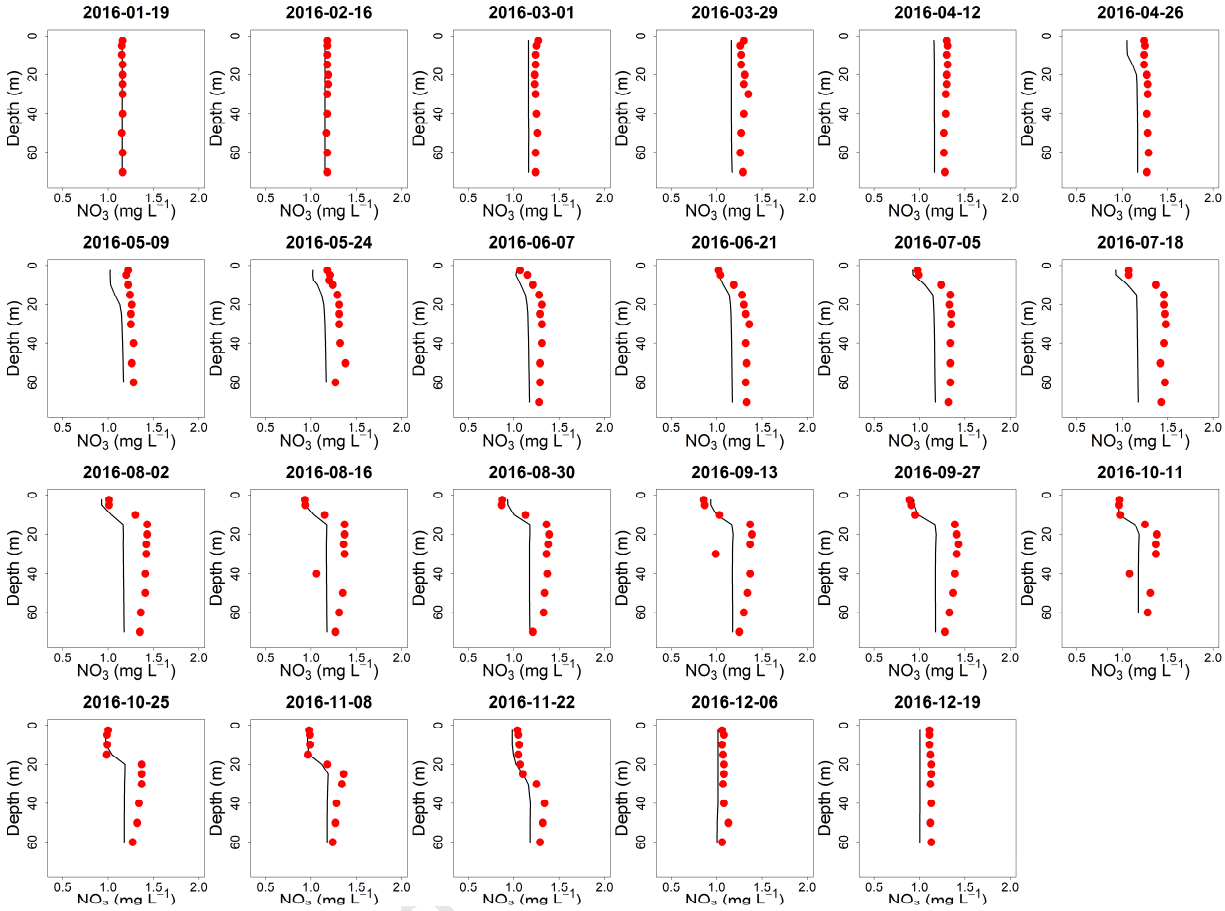

Figure 4. Comparison between simulation (black lines) and observation (red points) for NO_3 for different dates in 2016.

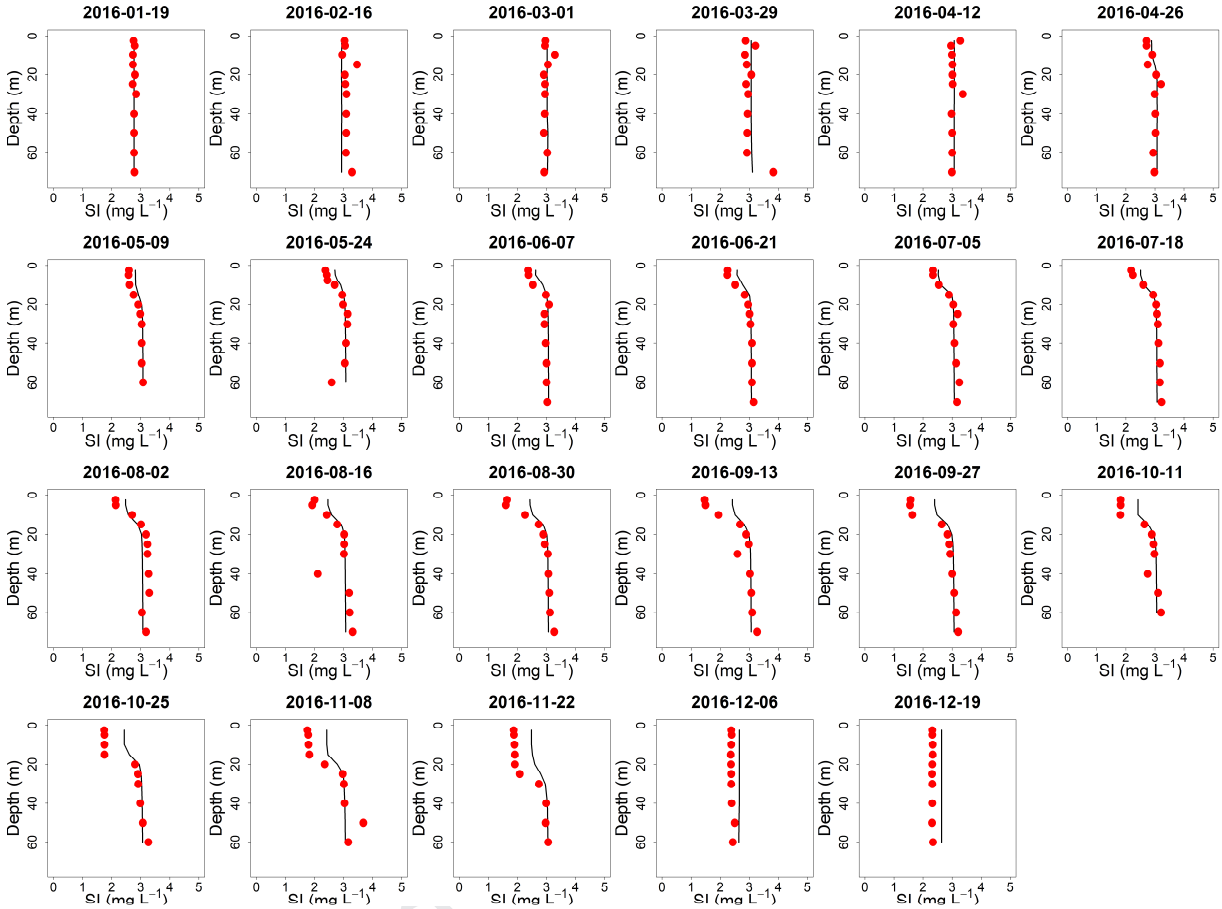

Figure 5. Comparison between simulation (black lines) and observation (red points) for silicate for different dates in 2016.

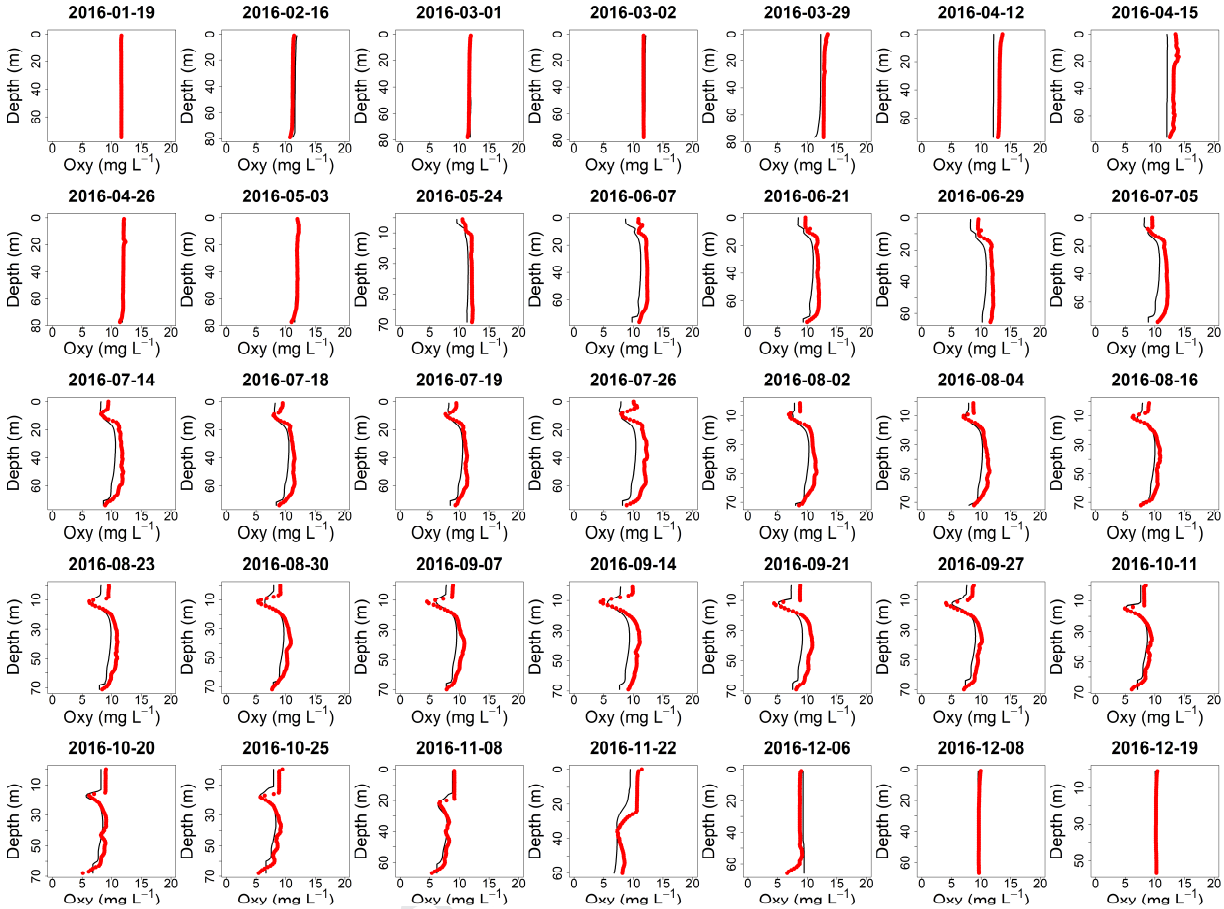

Figure 6. Comparison between simulation (black lines) and observation (red points) for oxygen for different dates in 2016.

.

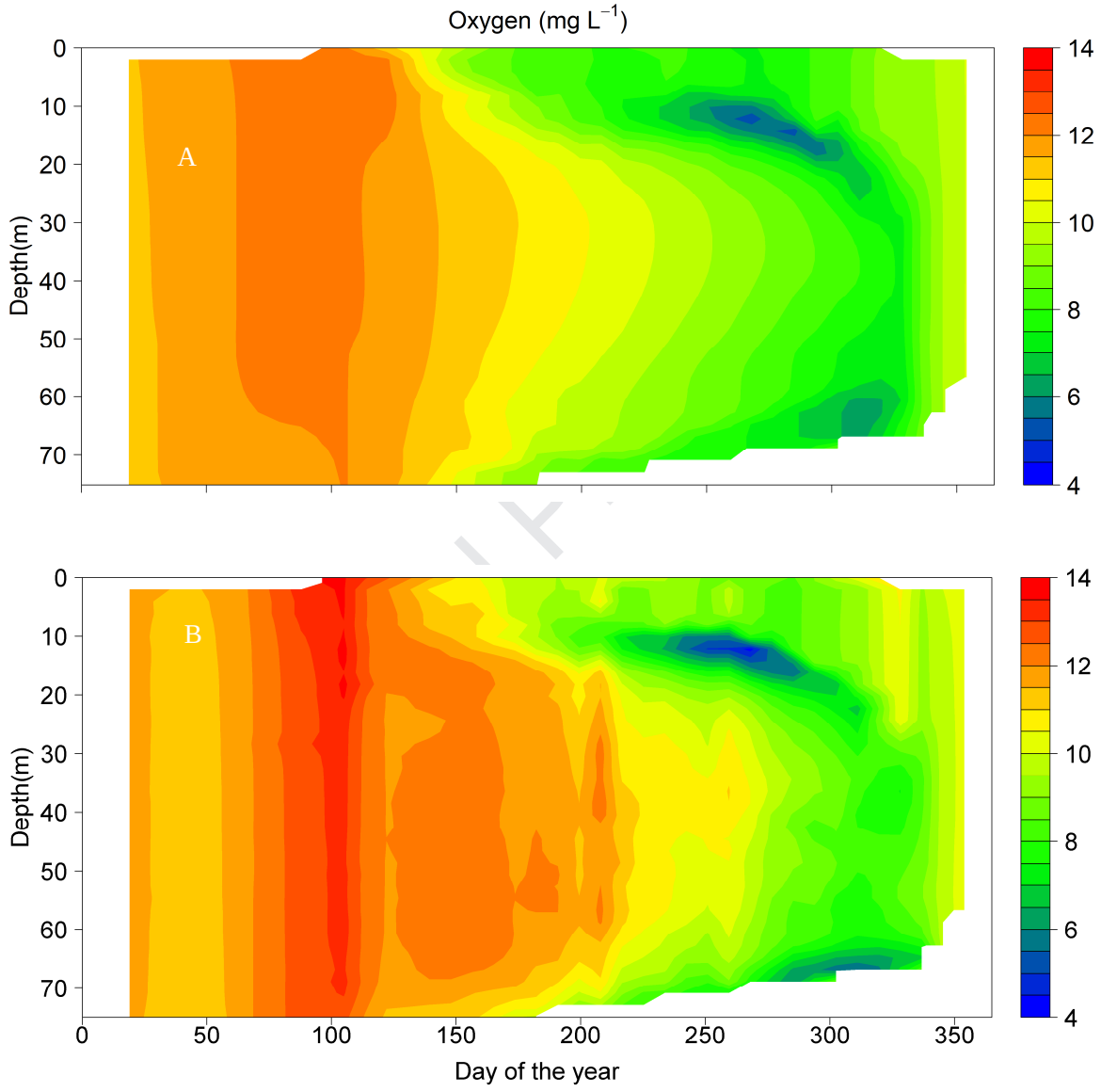

Figure 7. Comparison between simulation (A) and observation (B) for oxygen in 2016.

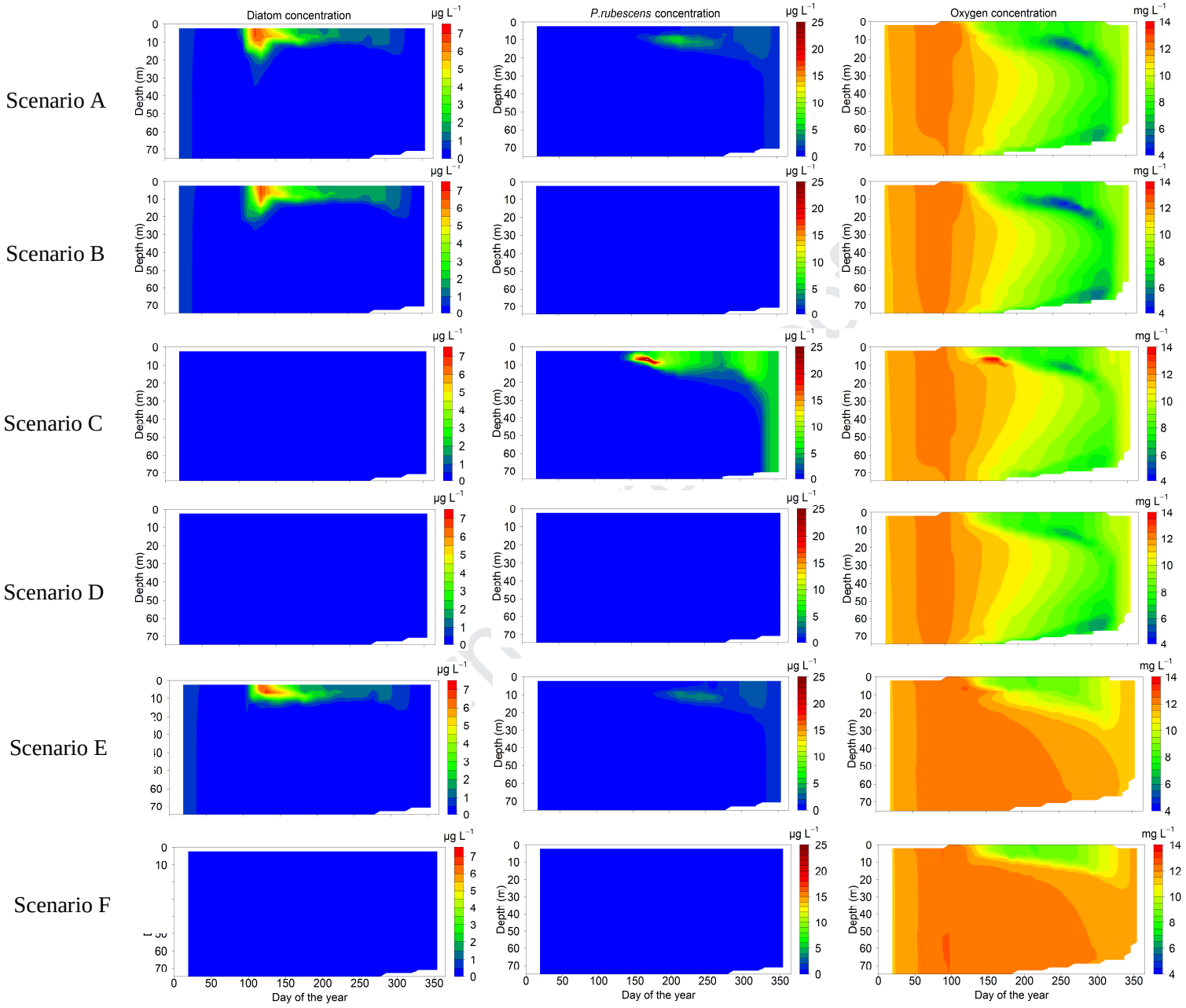

Figure 8. Simulated diatoms (left panels), *Planktothrix rubescens* (middle panels) and oxygen concentration (right panels) in different scenarios: (A) reference simulation, (B) as scenario A but without *P. rubescens*, (C) as scenario A but without diatoms, (D) as scenario A but without *P. rubescens* and diatoms, (E) as scenario A but with SOD=0, (F) as scenario D but with SOD=0.

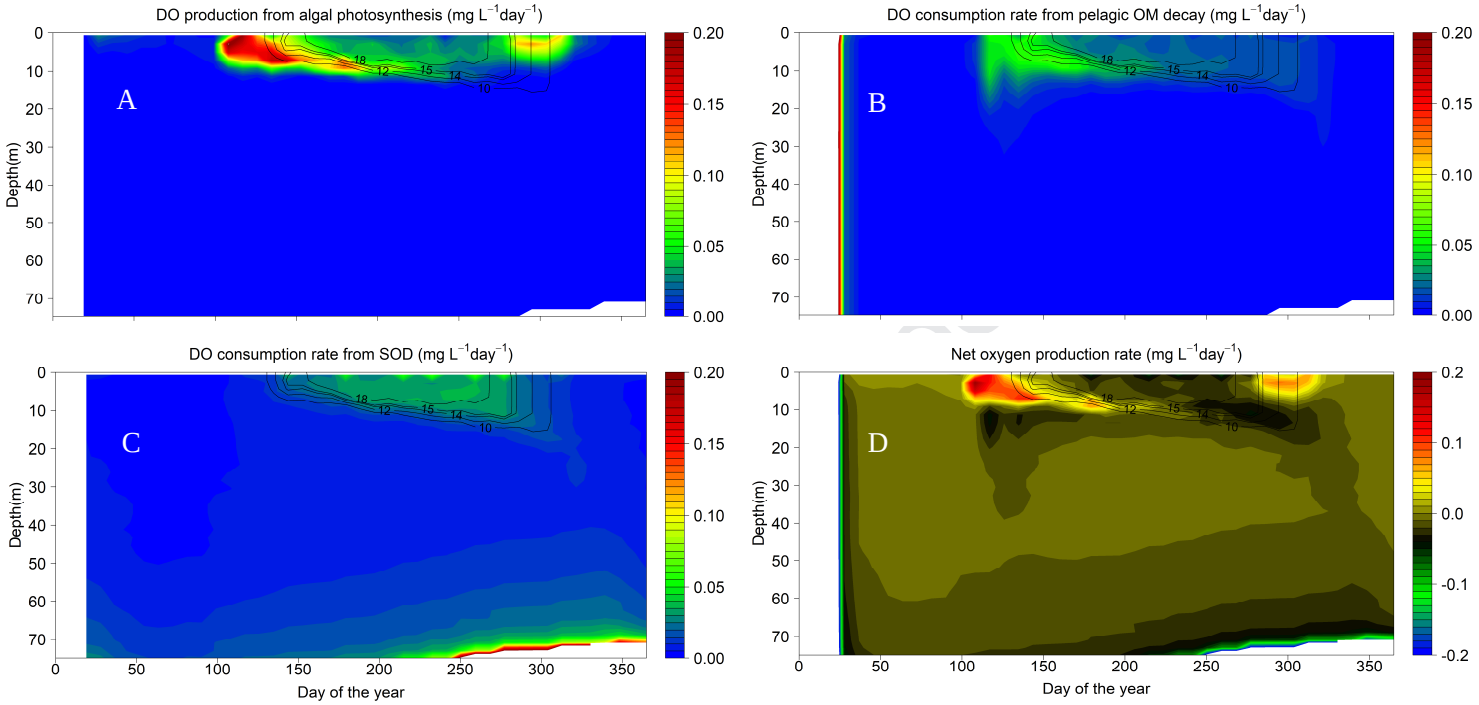

Figure 9. DO flux rate by different processes in the reference simulation: (A) by algal primary production, (B) by pelagic organic matter decay, (C) by SOD. Figure D indicates the net flux rate including all the three processes together (e.g. Figure D=Figure A-Figure B-Figure C). Contour lines are the simulated water temperature (°C).

Highlights

• The model accurately captured the metalimnetic oxygen minimum (MOM) in the reservoir

• Growth of *Planktothrix rubescens* delayed and slightly weakened the MOM

• Both pelagic and benthic oxygen depletion cause the MOM

• Water temperature in the metalimnion is decisive for MOM formation

Declaration of interests

☒ The authors declare that they have no known competing financial interests or personal relationships that could have appeared to influence the work reported in this paper.

☐The authors declare the following financial interests/personal relationships which may be considered as potential competing interests: